Nuclear Engineering and Technology 51 (2019) 221–227

Contents lists available at ScienceDirect

Nuclear Engineering and Technology

journal homepage: www.elsevier.com/locate/net

Original Article

Simulation of impact toughness with the effect of temperature and irradiation in steels

Chenchong Wang [a], Jinliang Wang [a], Yuhao Li [c], Chi Zhang [b], Wei Xu [a, *]

[a] State Key Laboratory of Rolling and Automation, School of Materials Science and Engineering, Northeastern University, Shenyang 110819, China
[b] Key Laboratory of Advanced Materials of Ministry of Education, School of Materials Science and Engineering, Tsinghua University, Beijing 100084, China
[c] High School Attached to Beijing University of Technology, Beijing 100022, China

ARTICLE INFO

Article history:
Received 26 February 2018
Received in revised form
2 August 2018
Accepted 21 August 2018
Available online 4 September 2018

Keywords:
Impact toughness
Simulation
Energy balance method
Temperature and irradiation

ABSTRACT

One of the important requirements for the application of reduced activation ferritic/martensitic steel is to retain proper mechanical properties in irradiation and high temperature conditions. In order to simulate the impact toughness with the effect of temperature and irradiation, a simulation model based on energy balance method consisted of crack initiation, plastic propagation and cleavage propagation stages was established. The effect of temperature on impact toughness was analyzed by the model and the trend of the simulation results was basicly consistent with the previous experimental results of CLAM steels. The load-displacement curve was simulated to express the low temperature ductile-brittle transition. The effect of grain size and inclusion was analyzed by the model, which was consistent with classical experiment results. The transgranular-intergranular transformation in brittle materials was also simulated.

1. Introduction

Reduced activation ferrite/martensite (RAFM) steels are considered as potential materials for first wall and blanket structure in international thermonuclear experimental reactor (ITER) [1–4]. In order to meet the application requirements for ITER, which contained irradiation and high temperature conditions, the impact toughness of RAFM steels was one of the critical properties, which would directly affect the service life of the reactor [5,6]. However, the experiment in irradiation and high temperature conditions was extremely difficult and costly. In order to reduce cost and guide the engineering project by theory, much attention was paid to analyze the mechanism and simulate steel's impact toughness in high temperature and irradiation conditions [7–10].

Several researches showed the experiment test results of RAFM's toughness [11–15]. In 2014, Baek et al. [11] reported the effect of temperature and irradiation on the fracture toughness in HT9 steel. Also, Huang et al. [12] reported the effect of temperature on impact toughness and ductile brittle transition temperature (DBTT) in China low activation martensitic (CLAM) steel. Recently, Park et al. [13] also studied the effect of isothermal aging time on the impact toughness of 9Cr–1WVTa RAFM steels. Although the toughness of RAFM steels was studied by various experiment researches, most of them just focused on the analysis of experiment results without establishment of models. The simulation of toughness in the field of steels was a long-standing problem. In 2016, Cho et al. [16] established a model to express the effect of precipitation on the impact toughness in high-carbon Cr–V tool steels. However, other factors except for precipitation were not considered in Cho's model. Also, several researchers tried to use finite element method (FEM) to simulate the impact toughness [17–20]. However, it was difficult for FEM to consider the effect of microstructure. Recently, XFEM models were widely used to simulate the relationship between microstructure and toughness of steels, however, most XFEM models could only show the effect of microstructure on crack propagation direction, instead of obtaining an accurate value of impact toughness [20].

In this work, a model based on the classical fracture theory and energy balance method was established to simulate the impact toughness of steels with the effect of temperature and irradiation. The model included different microstructure factors and could describe several traditional fracture phenomenon as low temperature ductile-brittle transition, irradiation hardening, transgranular-intergranular transformation, etc.

* Corresponding author.
E-mail address: xuwei@ral.neu.edu.cn (W. Xu).

https://doi.org/10.1016/j.net.2018.08.016

2. Simulation method

The model was mainly based on the energy balance method [21], which estimated the impact toughness by calculating the energy consumption in different fracture stages. According to the experiment analysis on the fracture mechanism, the fracture process of impact test could be divided into three stages [22]: (1) crack initiation; (2) plastic propagation of the crack; (3) cleavage propagation of the crack. So, the impact toughness could be expressed by Eq. (1).

$$E_{tot} = E_{int} + E_{plas} + E_{elas} \tag{1}$$

Where E_{int}, E_{plas} and E_{elas} were the energy consumption in crack initiation, plastic propagation and cleavage propagation stages, respectively. The simulation methods of E_{int}, E_{plas} and E_{elas} were introduced in detail below.

2.1. Energy consumption in crack initiation stage

The energy consumption in crack initiation stage was studied in the cohesive zone models [23,24]. Three typical traction-separation laws were used to express the relationship between load and displacement in crack initiation stage [25]: linear, polynomial and exponential function. Based on the three typical laws, the energy consumption in crack initiation stage could expressed by Eq. (2).

$$E_{int} = \int_0^{S_{int}} -\left(\frac{\sigma_{mas}}{S_{int}}\right)\cdot S + \sigma_{mas} = k_{int}\sigma_{mas}S_{int} \tag{2}$$

Where σ_{mas} was the maximal load during the impact process; S_{int} was the width of the crack initiation region (crack tip passivation); k_{int} was the integral coefficient of crack initiation stage.

The maximal load was proportional to the yield strength of the steel. Based on the experimental results and basic fracture toughness laws, constitutive equations were established to express σ_{mas} and S_{int} as Eqs. (3) and (4). In Eqs. (3) and (4), the effect of temperature, irradiation and inclusions were considered. And to simplify the simulation, the effect of temperature was supposed as a Gauss error function based on the experimental results [26,27]. The effect of irradiation and inclusions was simply supposed as a liner function, which can make this simulation avoid the complicated mechanism of irradiation defects temporarily.

$$\sigma_{mas} = a_m\sigma_0[erf(-\Delta T/n_{mas}) + 1]\left(1 - h_r\sum_i \chi_{m,i}\phi_i^{1/2}\right)(b_{mas}\Phi + c_{mas}) \tag{3}$$

$$S_{int} = a_{int}S_{int,0}[erf(\Delta T/n_{int}) + 1]\left(1 - h_r\sum_i \chi_{int,i}\phi_i^{2/3}\right)[erf(-\Delta\Phi/n_{int}) + 1] \tag{4}$$

Where ΔT was temperature increment(K)($T - 298(K)$); $\chi_{m,i}$ and $\chi_{int,i}$ were the weakening coefficient of inclusion i for load and displacement, respectively; Φ were irradiation damagement (dpa); σ_0 was initial load(N); $S_{int,0}$ was initial width of the crack initiation region; h_r was the interaction coefficient of inclusion weakening; $\Delta\Phi$ was relative irradiation damagement compared with critical effective irradiation damagement ($\Phi - 0.001$(dpa)). Other parameters were all equation correction coefficient.

2.2. Energy consumption in plastic propagation stage

Plastic propagation stage of the crack was also a process of crack tip passivation and crack propagation. So the energy consumption in plastic propagation stage was basicly similar with crack initiation stage and it could be expressed by Eq. (5) [25] and (6).

$$E_{plas} = \int_0^{S_{plas}} -\left(\frac{\sigma_{mas}}{S_{plas}^2}\right)\cdot S^2 + \sigma_{mas} = k_{plas}\sigma_{mas}S_{plas} \tag{5}$$

$$S_{plas} = a_p S_{p,0}[erf(\Delta T/m) + 1]\left(1 - h_r\sum_i \chi_{p,i}\phi_i^{2/3}\right)[erf(-\Delta\Phi/m) + 1] \tag{6}$$

Where $\chi_{p,i}$ was the weakening coefficient of inclusion i for the displacement in plastic propagation stage (fibrous crack length); k_{plas} was the integral coefficient of plastic propagation stage; m was equation correction coefficient.

2.3. Energy consumption in cleavage propagation stage

Based on cleavage fracture mechanism, the energy consumption in cleavage propagation stage was expressed by Eq. (7), which was based on superposition law. And the resistance of grain boundary term was defined base on the mechanism of Hall-Petch relation.

$$E_{elas} = A_c\left[f_b\gamma_b + (1 - f_b)\left(\gamma_c + \kappa d^{-2}\right)\right] \tag{7}$$

Where A_c was the area of fracture surface (cm^2); f_b was the fraction of grain boundary crack; γ_b and γ_c were the decohesive energy of grain boundary and crystal crack (J/cm2), respectively; κ was the resistance coefficient of grain boundary (J); d was the grain size (μm).

Based on Eq. (7), the energy consumption in cleavage propagation stage was divided into two parts: grain boundary crack (intergranular) and crystal crack (transgranular). For the part of crystal crack, the resistance of grain boundary was considered to express the effect of grain size. The difference between decohesive energy of grain boundary and crystal crack were the gradient criterion of intergranular and transgranular crack. The crack preferred to propagate along the direction with lowest energy consumption, so the fraction of grain boundary crack could be expressed by Gauss error function as Eq. (8) [28], traditional mathematical treatment for gradient criterion. And constitutive equations were also established to express the decohesive energy of grain boundary and crystal crack as Eqs. (9) and (10).

$$f_b = erf\left(\frac{\gamma_c}{\gamma_b}\right) \tag{8}$$

$$\gamma_c = a_c\gamma_{c,0}[erf(-\Delta T/c) + 1]\left(1 - h_r\sum_i \chi_{c,i}\phi_i^{2/3}\right)(b_c\Phi + c_c) \tag{9}$$

$$\gamma_b = a_b\gamma_{b,0}[erf(-\Delta T/b) + 1]\left(1 - h_r\sum_i \chi_{b,i}\phi_i d/r_i\right)(b_b\Phi + c_b) \tag{10}$$

Where $\chi_{c,i}$ and $\chi_{b,i}$ were the weakening coefficient of inclusion i for

Table 1
Value of the parameters used in the model.

Parameter	Value	Parameter	Value
a_m, a_{int}, a_p	0.5[a]	κ	1×10^8[a]
σ_0	40 kN[b]	A_0	1 cm^2[b]
$S_{int,0}$	4 mm[b]	θ	45°[b]
$S_{p,0}$	14 mm[b]	a_c,a_b	0.5[a]
n_{mas}, n_{int}	80[c]	b	100[a]
h_r	1.21[c]	c	200[a]
$\chi_{m,i}$, $\chi_{int,i}$, $\chi_{p,i}$	0.5[a]	$\chi_{c,i}$	0.5[a]
b_{mas}, b_c, b_b	0.01[c]	$\chi_{b,i}$	0.3[a]
$\gamma_{c,0}$	20J/cm^2[a]	$\gamma_{b,0}$	35 J/cm^2[a]
c_{mas}, c_c, c_b	1[c]	m	80[c]

[a] Obtained from classical constant or subjective experience.
[b] Obtained from experiment results in Refs. [9,13–15,18,22].
[c] Obtained from fitting.

the transgranular and intergranular crack in cleavage propagation stage, respectively; $\gamma_{c,0}$ and $\gamma_{b,0}$ were the initial decohesive energy of grain boundary and crystal crack, respectively.

In cleavage propagation stage, the crack propagation process would finish in extremely short time and the crack propagation path has certain randomness. Based on the geometric relation, the distance of crack propagation path would only be affected by the bending angle, instead of the bending times. So, the area of fracture surface (A_c) was set as a range from A_0 to $A_0/\cos\theta$. A_0 represented the cross-sectional area of the impact samples. θ represented the maximum bending angle. Because of the uncertainty of A_c, the calculation results of impact toughness would be a range (as error band), instead of an accurate value. The calculation results with an error band were more reasonable than an accurate value, because the experiment results of impact toughness were also unstable. For this model, the error band calculation was only based on the uncertainty in the direction of crack propagation. However, the experimental error of impact toughness was from not only the uncertainty in the direction of crack propagation, but also the surface quality of the sample, the machining precision of notch, etc., which were difficult to explain by models. So the experiment value would probably have difference with the simulated error band.

3. Results and discussion

Table 1 showed the parameters used in the model. The optimized value of the fitting parameters was obtained by cycle optimization based on the method of exhaustion. The initial grain size was set as 5 μm. The simulation results of load-displacement curve were shown in Fig. 1. The simulation results indicated that the decrease of temperature mainly affect the width of the crack initiation region and plastic propagation region. The material was difficult to obtain an obvious crack passivation zone when the

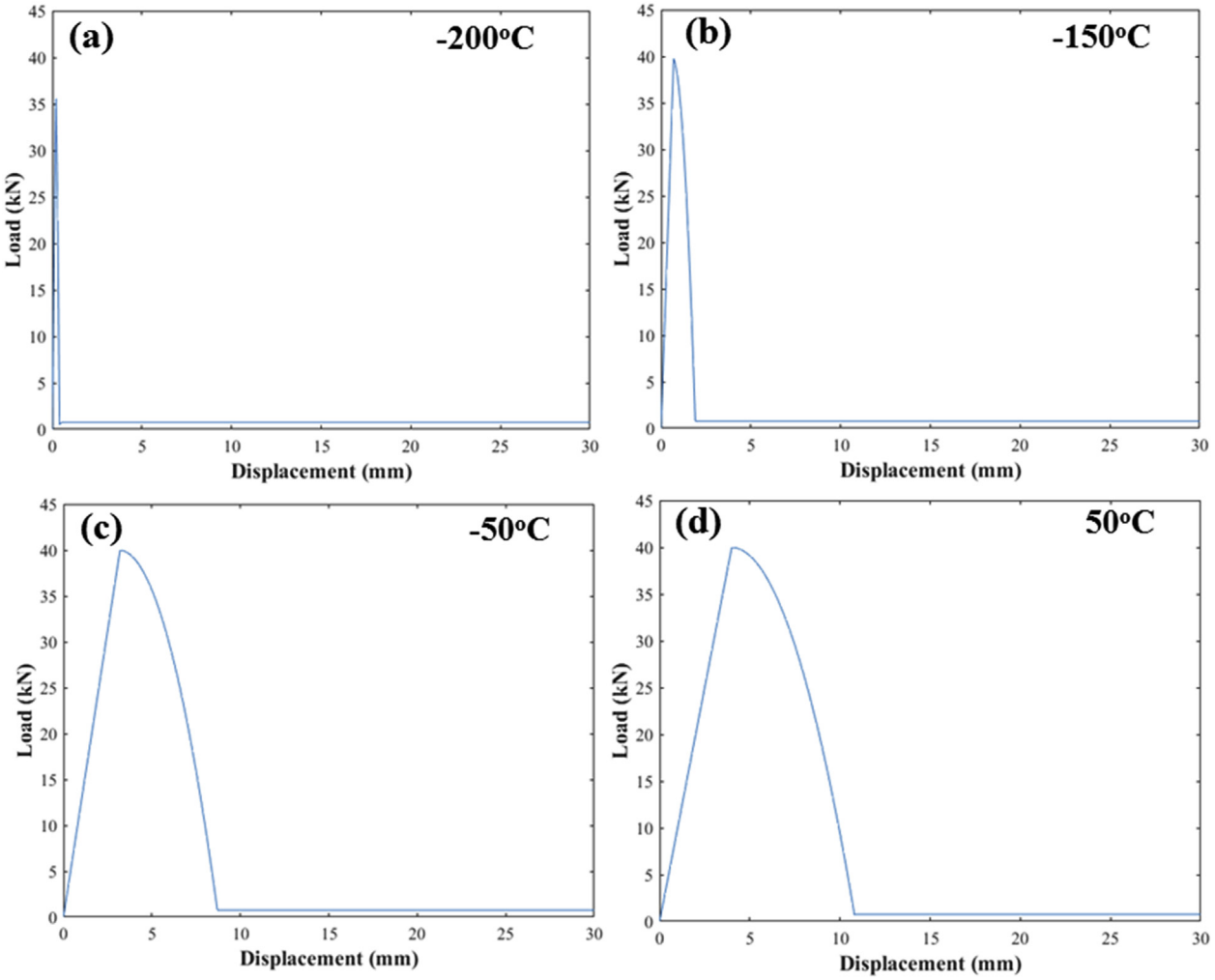

Fig. 1. Simulation results of load-displacement curve without irradiation: (a) −200 °C; (b) −150 °C; (c) −50 °C; (d) 50 °C.

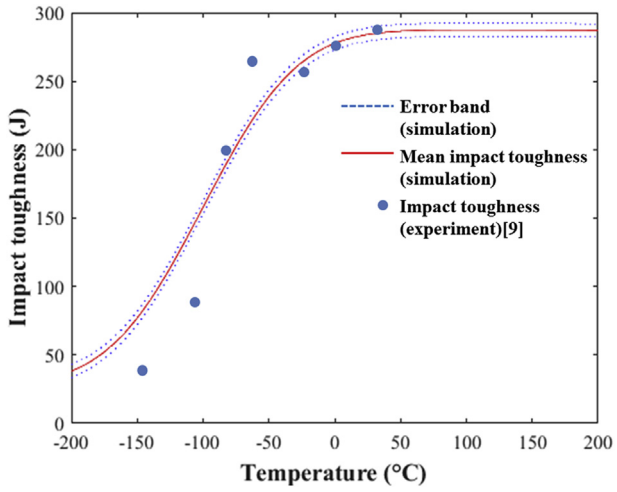

Fig. 2. Effect of temperature on impact toughness of CLAM steel without irradiation.

temperature was lower than −150 °C. With the decrease of temperature, the crack passivation and plastic propagation zone was greatly decreased, which represented the phenomenon of low temperature ductile-brittle transition. Fig. 2 showed the effect of temperature on the impact toughness simulated by the model. The trend of the simulation results was basicly consistent with the previous experimental results of CLAM steels [9].

Fig. 3 showed the effect of irradiation on the impact toughness. The simulation results indicated that with the increase of irradiation damage, the toughness decreased (Fig. 3(a)). The crack passivation and plastic propagation zone in low and high irradiation condition were compared in Fig. 3(b) and (c). Based on the simulation results, the irradiation didn't decrease the maximal load, but it decreased the width of the crack initiation region and plastic propagation region significantly. So, the material was difficult to obtain an obvious crack passivation zone. The decrease of toughness by irradiation was mainly caused by the decrease of crack passivation and plastic propagation zone, which was consistent with the well-known irradiation hardening phenomenon. As shown in Fig. 3(a), the simulation results were basically consistent with the experimental results by Q. Huang's research with low level irradiation (<1.5dpa) [13]. It meant that this model had its reasonability. However, because of the limitation of irradiation source, the experimental test of the impact toughness with irradiation effect was still a difficult work with large data dispersity. Much more experimental data was still needed to estimate the accuracy of this model. However, this model provided a method to simulate the impact toughness of RAFM steels with the effect of low level irradiation, and it partly showed the mechanism that irradiation decreased the impact toughness of the steels by decreasing the crack passivation and plastic propagation zone.

Other traditional fracture phenomenon could also be indicated by this model besides the effect of temperature and irradiation. Fig. 4(a) showed the effect of grain size on the impact toughness in brittle materials (the width of crack initiation and plastic

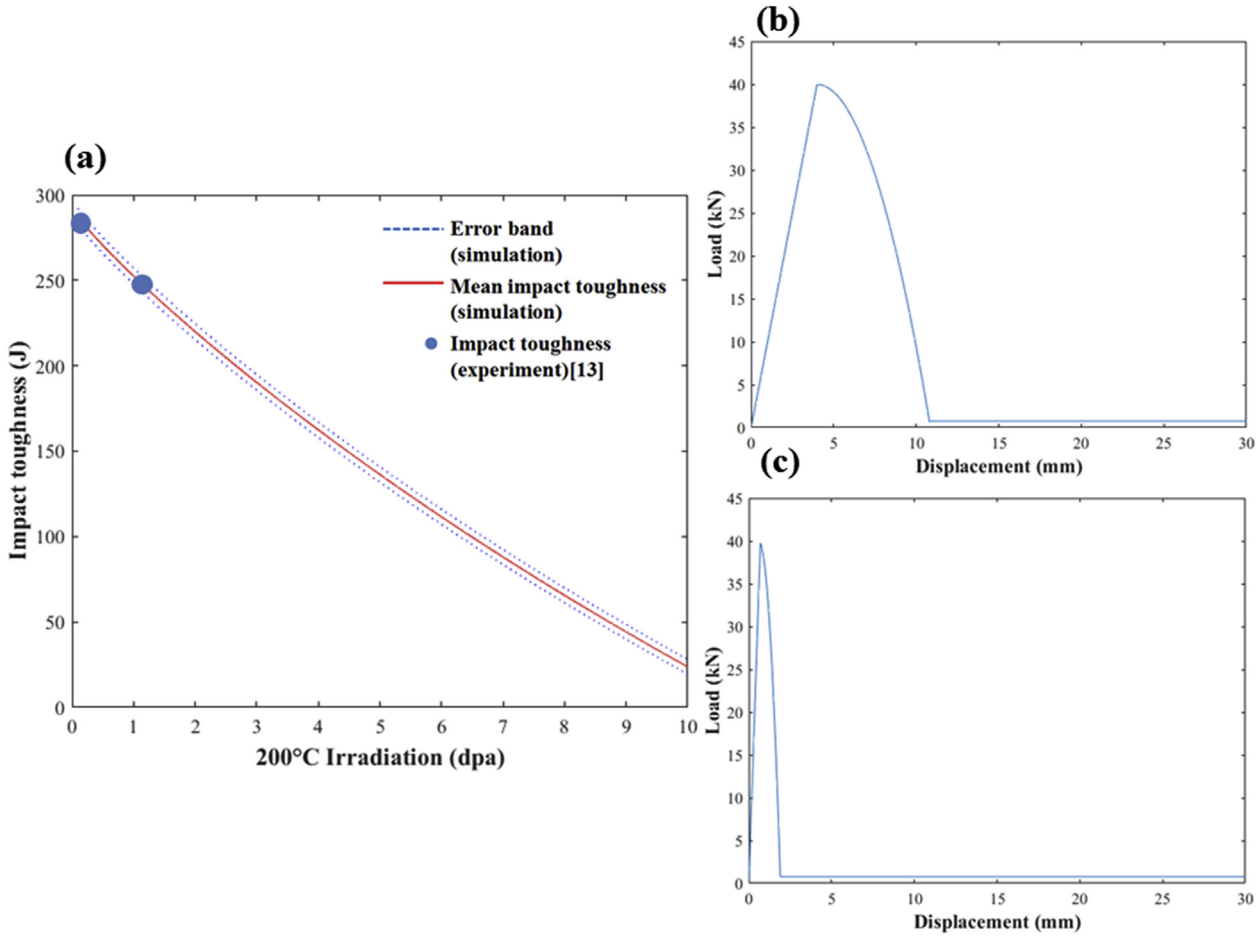

Fig. 3. Simulation of irradiation effect on impact toughness: (a) irradiation effect on impact toughness; (b) load-displacement curve for 0dpa; (c) load-displacement curve for 5dpa.

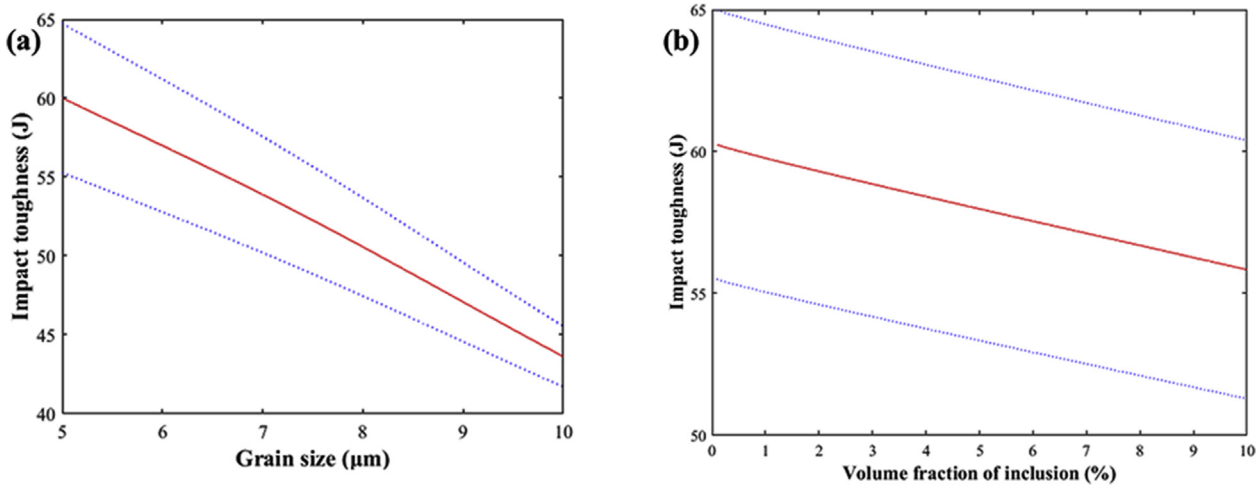

Fig. 4. Simulation of microstructure effect on impact toughness at room temperature without irradiation: (a) grain size effect; (b) inclusion effect.

propagation region was both less than 0.5 mm). The results showed that the impact toughness decreased by grain coarsening, which was consistent with the classical grain refinement theory [29,30]. Fig. 4(b) showed the effect of inclusions on the impact toughness in brittle materials, which indicated that the increase of inclusion content was bad for the impact toughness of brittle materials, which was also consistent with experiment results [31,32].

The model could also describe transgranular-intergranular transition phenomenon in brittle material. Fig. 5(a) showed that the increase of inclusion content at the grain boundary would greatly reduce the decohesive energy of the grain boundary. So, the crack propagation mode would gradually change from transgranular to intergranular when the decohesive energy of the grain boundary became lower than crystal (Fig. 5(b)). The transgranular-

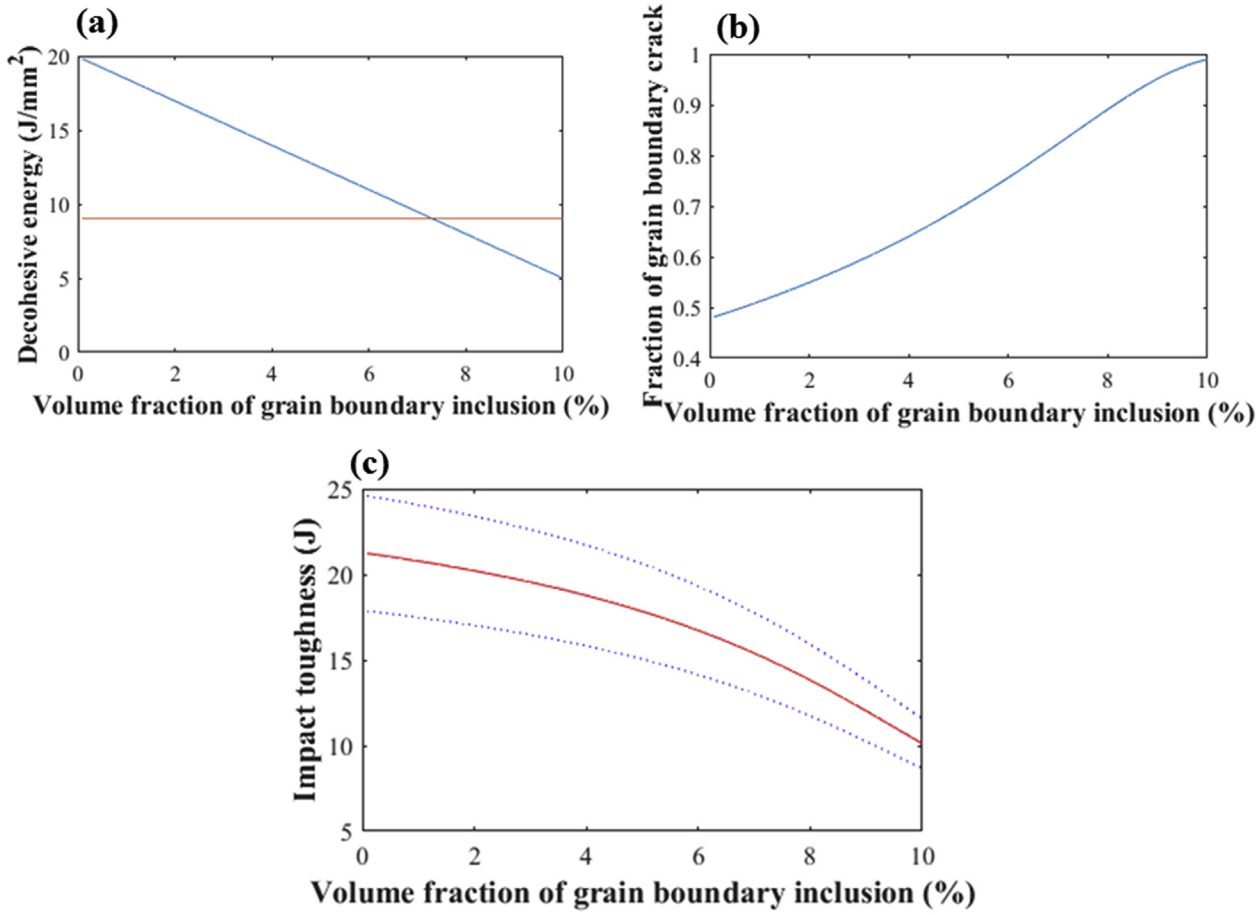

Fig. 5. Simulation of transgranular-intergranular transformation without irradiation: (a) decohesive energy; (b) fraction of grain boundary crack; (c) impact toughness.

intergranular transition phenomenon finally led to the significant decrease of impact toughness in brittle material, which was also shown in the simulation results (Fig. 5(c)).

In this impact toughness simulation model, the equations used to express the width of the crack initiation and plastic propagation regions were still semi-empirical equations, which meant the mechanism of alloy's plastic deformation were still unclear in this model. Also, based on these semi-empirical equations, this model could describe the phenomenon of low temperature ductile-brittle transition, but couldn't explain the physical mechanism. Also, part of the parameters values in this model were still based on fitting results, which would inhibit the predictability and application scope of this model. The assumption of the linear effect of dpa from irradiation in this model would probably be different with the actual situation, especially when the irradiation was in relatively high level. Therefore, when using this model to a high level irradiation condition (>10dpa), any conclusion regarding the effect of irradiation from the model should be cautious and the modification of the irradiation effect on defects and properties was necessary. In order to widen the application of this model, more modification should be made to establish the model, which could accurately express the effect of irradiation on defects (He bubbles and dislocation loops) and the effect of defects on plasticity. Impact toughness simulation was a long-standing problem, which couldn't be completely solved by one paper. However, this model established a framework of impact toughness simulation with the effect of temperature and irradiation and provided a feasible way for future research. Also, this model provides an algorithm of cleavage propagation crack based on the mechanism of brittle fracture, which could explain several classical cleavage fracture phenomenon, including transgranular-intergranular transition. Because of the limitation of parameter accuracy, this model is suggested to be used in the field of RAFM steels with irradiation less than 10dpa and temperature between −200 °C and 200 °C. If further studies planned to use this model in the field of other metal materials, much more effort should be made to optimize parameter values.

4. Conclusion

A constitutive model based on energy balance method was established to calculate the impact toughness of steels with the effect of temperature and irradiation. The model contained crack initiation, plastic propagation and cleavage propagation stages, which was consistent with the classical fracture theory. The model can simulate the load-displacement curve of the impact test. Using this model, the effect of temperature on impact toughness was analyzed and the trend of the simulation results was basicly consistent with the previous experimental results of CLAM steels. The model included different microstructure factors and could describe several traditional fracture phenomenon as low temperature ductile-brittle transition, irradiation hardening, transgranular-intergranular transformation et al. This model established a framework of impact toughness simulation with the effect of temperature and irradiation and provided a feasible way for future research.

Acknowledgements

This work was financially supported by the National Natural Science Foundation of China (Grant No. 51574080). Greatly acknowledged the financial support provided by Basic scientific research funds of Northeastern University (N160705002). The authors acknowledge the assistance of Beijing Academy of Science and Technology Innovation for Teenagers with the modeling and simulation.

Appendix A. Supplementary data

Supplementary data related to this article can be found at https://doi.org/10.1016/j.net.2018.08.016.

References

[1] T.K. Kim, S. Noh, S.H. Kang, J.J. Park, H.J. Jin, M.K. Lee, J. Jang, C.K. Rhee, Current status and future prospective of advanced radiation resistant oxide dispersion strengthened steel (ARROS) development for nuclear reactor system applications, Nucl. Eng. Technol. 48 (2016) 572–594.
[2] C. Wang, C. Zhang, J. Zhao, Z. Yang, W. Liu, Microstructure evolution and yield strength of CLAM steel in low irradiation condition, Mater. Sci. Eng. A 682 (2017) 563–568.
[3] W. Wang, S. Liu, G. Xu, B. Zhang, Q. Huang, Effect of thermal aging on microstructure and mechanical properties of China low-activation martensitic steel at 550 degrees C, Nucl. Eng. Technol. 48 (2016) 518–524.
[4] S.N. Zhu, C. Zhang, Z.G. Yang, C.C. Wang, Hydrogen's influence on reduced activation ferritic/martensitic steels' elastic properties: density functional theory combined with experiment, Nucl. Eng. Technol. 49 (2017) 1748–1751.
[5] C. Wang, C. Zhang, Z. Yang, J. Zhao, Multiscale simulation of yield strength in reduced-activation ferritic/martensitic steel, Nucl. Eng. Technol. 49 (2017) 569–575.
[6] Y.-Y. Wang, J.-H. Ding, W.-B. Liu, S.-S. Huang, X.-Q. Ke, Y.-Z. Wang, C. Zhang, J.-J. Zhao, Irradiation-induced void evolution in iron: a phase-field approach with atomistic derived parameters, Chin. Phys. B (2017) 26.
[7] J. Brnic, G. Turkalj, M. Canadija, S. Krscanski, M. Brcic, D. Lanc, Deformation behaviour and material properties of austenitic heat-resistant steel X15CrNiSi25-20 subjected to high temperatures and creep, Mater. Des. 69 (2015) 219–229.
[8] C.C. Eiselt, H. Schendzielorz, A. Seubert, B. Hary, Y. de Carlan, P. Diano, B. Perrin, D. Cedat, ODS-materials for high temperature applications in advanced nuclear systems, Nucl. Mater. Energy 9 (2016) 22–28.
[9] W. Wang, J. Chen, G. Xu, Effect of thermal aging on grain structural characteristic and Ductile-to-Brittle transition temperature of CLAM steel at 550°C, Fusion Eng. Des. 115 (2017) 74–79.
[10] S.J. Zinkle, J.L. Boutard, D.T. Hoelzer, A. Kimura, R. Lindau, G.R. Odette, M. Rieth, L. Tan, H. Tanigawa, Development of next generation tempered and ODS reduced activation ferritic/martensitic steels for fusion energy applications, Nucl. Fusion 57 (2017).
[11] J.-H. Baek, T.S. Byun, S.A. Maloy, M.B. Toloczko, Investigation of temperature dependence of fracture toughness in high-dose HT9 steel using small-specimen reuse technique, J. Nucl. Mater. 444 (2014) 206–213.
[12] X. Chen, Y. Huang, B. Madigan, J. Zhou, An overview of the welding technologies of CLAM steels for fusion application, Fusion Eng. Des. 87 (2012) 1639–1646.
[13] Q. Huang, Development status of CLAM steel for fusion application, J. Nucl. Mater. 455 (2014) 649–654.
[14] M.G. Park, C.H. Lee, J. Moon, J.Y. Park, T.-H. Lee, N. Kang, H. Chan Kim, Effect of microstructural evolution by isothermal aging on the mechanical properties of 9Cr-1WVTa reduced activation ferritic/martensitic steels, J. Nucl. Mater. 485 (2017) 15–22.
[15] L. Tan, Y. Katoh, A.A.F. Tavassoli, J. Henry, M. Rieth, H. Sakasegawa, H. Tanigawa, Q. Huang, Recent status and improvement of reduced-activation ferritic-martensitic steels for high-temperature service, J. Nucl. Mater. 479 (2016) 515–523.
[16] K.S. Cho, S.I. Kim, S.S. Park, W.S. Choi, H.K. Moon, H. Kwon, Effect of Ti addition on carbide modification and the microscopic simulation of impact toughness in high-carbon Cr-V tool steels, Metall. Mater. Trans. A 47 (2015) 26–32.
[17] N.A. Giang, M. Kuna, G. Huetter, Influence of carbide particles on crack initiation and propagation with competing ductile-brittle transition in ferritic steel, Theor. Appl. Fract. Mech. 92 (2017) 89–98.
[18] J.E. Jam, M. Abolghasemzadeh, H. Salavati, Y. Alizadeh, The effect of notch tip position on the charpy impact energy for bainitic and martensitic functionally graded steels, Strength Mater. 46 (2014) 700–716.
[19] R. Wu, J. Li, Y. Su, S. Liu, Z. Yu, Improved uniformity of hardness by continuous low temperature bainitic transformation in prehardened mold steel with large section, Mater. Sci. Eng. A 706 (2017) 15–21.
[20] C. Wang, C. Zhang, Z. Yang, J. Su, Y. Weng, Analysis of fracture toughness in high Co–Ni secondary hardening steel using FEM, Mater. Sci. Eng. A 646 (2015) 1–7.
[21] G. Seisson, D. Hébert, I. Bertron, J.M. Chevalier, L. Hallo, E. Lescoute, L. Videau, P. Combis, F. Guillet, M. Boustie, L. Berthe, Dynamic cratering of graphite: experimental results and simulations, Int. J. Impact Eng. 63 (2014) 18–28.
[22] R. Cao, J. Li, D.S. Liu, J.Y. Ma, J.H. Chen, Micromechanism of decrease of impact toughness in coarse-grain heat-affected zone of HSLA steel with increasing welding heat input, Metall. Mater. Trans. A 46 (2015) 2999–3014.
[23] V. Carollo, J. Reinoso, M. Paggi, A 3D finite strain model for intralayer and interlayer crack simulation coupling the phase field approach and cohesive zone model, Comps. Struct. 182 (2017) 636–651.
[24] Y. Xu, Y. Guo, L. Liang, Y. Liu, X. Wang, A unified cohesive zone model for simulating adhesive failure of composite structures and its parameter identification, Comps. Struct. 182 (2017) 555–565.

[25] A. Pineau, Modeling ductile to brittle fracture transition in steels—micromechanical and physical challenges, Int. J. Fract. 150 (2008) 129–156.
[26] H. Zhang, S. Li, G. Liu, Y. Wang, Effects of hot working on the microstructure and thermal ageing impact fracture behaviors of Z3CN20-09M duplex stainless steel, Acta Metall. Sin. 53 (2017) 531–538.
[27] S.S.M. Tavares, M.B. Silva, M.C.S. de Macedo, T.R. Strohaecker, V.M. Costa, Characterization of fracture behavior of a Ti alloyed supermartensitic 12%Cr stainless steel using Charpy instrumented impact tests, Eng. Fail. Anal. 82 (2017) 695–702.
[28] M. Perez, M. Dumont, D. Acevedo-Reyes, Implementation of classical nucleation and growth theories for precipitation, Acta Mater. 56 (2008) 2119–2132.
[29] P. Wang, F. Liu, Y.P. Lu, C.L. Yang, G.C. Yang, Y.H. Zhou, Grain refinement and coarsening in hypercooled solidification of eutectic alloy, J. Cryst. Growth 310 (2008) 4309–4313.
[30] C. Wang, C. Zhang, Z. Yang, J. Su, Y. Weng, Microstructure analysis and yield strength simulation in high Co–Ni secondary hardening steel, Mater. Sci. Eng. A 669 (2016) 312–317.
[31] P.V. Bizyukov, S.R. Giese, Effects of Zr, Ti, and Al additions on nonmetallic inclusions and impact toughness of cast low-alloy steel, J. Mater. Eng. Perform. 26 (2017) 1878–1889.
[32] A. Ghosh, P. Modak, R. Dutta, D. Chakrabarti, Effect of MnS inclusion and crystallographic texture on anisotropy in Charpy impact toughness of low carbon ferritic steel, Mater. Sci. Eng. A 654 (2016) 298–308.